Source directivity in the wave based WRWes simulation

Rob Opdam[1], Diemer de Vries[1], Michael Vorländer[1]

[1] *RWTH Aachen University, 52074 Aachen, Germany, Email: rob.opdam@akustik.rwth-aachen.de*

Introduction

In this paper the WRWes algorithm [1, 2] is extended with the option to include a measured source directivity in a room acoustic simulation. The idea is to have the possibility to include measured directivities in a type of boundary element method simulation. The advantage is to remove the need of a geometrical model of the sound source and to simulate for instance the surface velocities by a structural simulation. In this way only a simulation of the fluid domain is necessary. The source will be a monopole with a frequency and direction dependent complex weighting factors mapped on to it to represent the original directivity of a source. First the WRWes algorithm will be briefly explained and then the extension of including of measured directivities.

Theory WRWes

The WRWes model is based on the Rayleigh-II Integral, that states that in every point in the volume V of Figure 1 the complex pressure P can be calculated if the primary sources are located below or on the boundary plane S_1. The Rayleigh-II integral can be derived from the

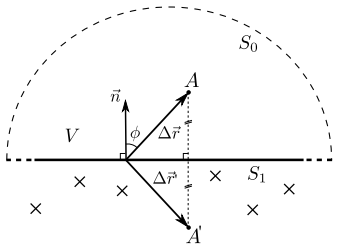

Figure 1: Rayleigh integral equation domain with primary sources (×), volume V and boundary $S = S_0 + S_1$.

Kirchhoff-Helmholtz equation and Green's second theorem [3] and is formulated in 2-D as:

$$P(\vec{r}_A,\omega) = \frac{jk}{2\pi}\int\limits_{S_1} P(\vec{r}_{S_1},\omega)H_1^{(2)}(k|\Delta\vec{r}|)\cos(\phi)dS_1 \quad (1)$$

and in 3-D as:

$$P(\vec{r}_A,\omega) = \frac{1}{2\pi}\int\limits_{S_1} P(\vec{r}_{S_1},\omega)\frac{1+jk|\Delta\vec{r}|}{|\Delta\vec{r}|^2}e^{-jk|\Delta\vec{r}|}\cos(\phi)dS_1, \quad (2)$$

where P is the complex pressure, $H_1^{(2)}$ is the the first order Hankel function of the second kind, $|\Delta\vec{r}| = |\vec{r}_A - \vec{r}_S|$ is the distance from a secondary source point on the boundary S_1 to the reconstruction point A within the enclosed volume V, ϕ is the angle between the normal vector $\vec{n}$ pointing inward to the volume and the vector $\vec{\Delta r}$ between a secondary source and the reconstruction point. The wavenumber k is defined as the angular frequency ω divided by the propagation velocity c.

The Rayleigh-II integral equation can be written as the integral over a kernel $W(|\Delta\vec{r}|,\omega)$ and the secondary source pressure $P(\vec{r}_{S_1},\omega)$ at the boundary S_1:

$$P(\vec{r}_A,\omega) = \int\limits_{S_1} W(|\Delta\vec{r}|,\omega)P(\vec{r}_{S_1},\omega)dS_1, \quad (3)$$

with as 2-D kernel:

$$W_{\text{2-D}}(|\Delta\vec{r}|,\omega) = \frac{jk}{2\pi}H_1^{(2)}(k|\Delta\vec{r}|)\cos(\phi), \quad (4)$$

and 3-D kernel:

$$W_{\text{3-D}}(|\Delta\vec{r}|,\omega) = \frac{1+jk|\Delta\vec{r}|}{4\pi|\Delta\vec{r}|^2}e^{-jk|\Delta\vec{r}|}\cos(\phi). \quad (5)$$

In discrete formulation this integral can be evaluated by a matrix multiplication of a matrix $\mathbf{W}$ and a vector $\vec{P}_{S_1}$:

$$\vec{P} = \mathbf{W}\vec{P}_{S_1} \quad (6)$$

The propagation from one boundary as demonstrated above is extended to an enclosed geometry. Therefore the notation of the matrices will be defined as follows: the lower indices of the matrices indicate the propagation direction, for example $\mathbf{W}_{ds}$ for the propagation from the source(s) to the detector(s), or the boundary they are working on, for example $\mathbf{R}_{b_1}$. The configuration of the boundaries is unrestricted and does not even have to be closed, but should be on total convex. The example case that is used is a rectangular room with four sidewalls (boundaries b_1 to b_4), which also encloses the sources (s_1 and s_2) and detectors (d_1 to d_4) as shown in Figure 2. The contribution to the wave field by the reflective

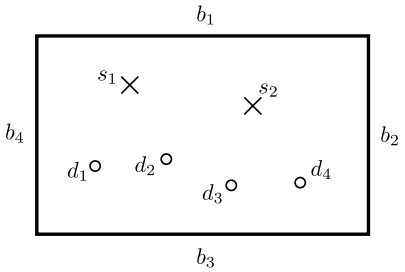

Figure 2: Rectangular room with walls (boundaries), sources (×) and detectors (○).

part can be defined as an iterative process, which starts with propagation from the sources to the walls followed

by a reflection and propagation to the other walls and finally reaches the detector points. The calculation of the reflected wave field is schematically shown in the top part of Figure 3. The matrix operators that include all

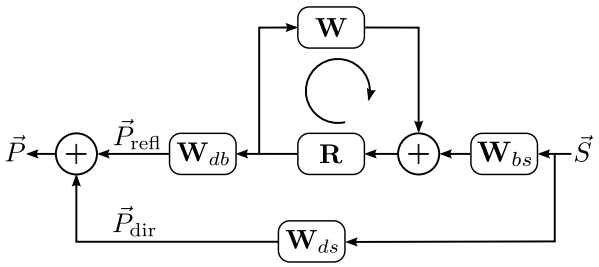

Figure 3: Diagram of the model with the total $\vec{P}$, reflected $\vec{P}_{\text{refl}}$ and direct wave field $\vec{P}_{\text{dir}}$.

the reflection and propagation properties for the complete geometry are defined as follows. The source vector $\vec{S}$ includes the number of sources and their strength for the specific frequency ω and is defined as (with the total number of sources i):

$$\vec{S} = \begin{pmatrix} S_1(\omega) & S_2(\omega) & \cdots & S_i(\omega) \end{pmatrix}^T. \tag{7}$$

The matrix operator for the propagation from sources to detectors $\mathbf{W}_{ds}$, sources to the boundaries $\mathbf{W}_{bs}$ and boundaries to the detector(s) $\mathbf{W}_{db}$ are defined as (with the total number of sources, detectors and/or boundaries indicated as i and j):

$$\mathbf{W}_{xy} = \begin{pmatrix} W_{x_1y_1} & W_{x_1y_2} & \cdots & W_{x_1y_i} \\ W_{x_2y_1} & W_{x_2y_2} & \cdots & W_{x_2y_i} \\ \vdots & \vdots & \ddots & \vdots \\ W_{x_jy_1} & W_{x_jy_2} & \cdots & W_{x_jy_i} \end{pmatrix}. \tag{8}$$

The boundary properties are collected in one matrix $\mathbf{R}$, where on the diagonal the matrices of separate boundary properties $\mathbf{R}_b$, as mentioned above, are placed:

$$\mathbf{R} = \begin{pmatrix} \mathbf{R}_{b_1} & \mathbf{0} & \cdots & \mathbf{0} \\ \mathbf{0} & \mathbf{R}_{b_2} & & \vdots \\ \vdots & & \ddots & \mathbf{0} \\ \mathbf{0} & \cdots & \mathbf{0} & \mathbf{R}_{b_N} \end{pmatrix}. \tag{9}$$

Propagation between boundaries is collected in the matrix $\mathbf{W}$, which includes the individual propagations between the boundary parts (with N the total number of boundaries):

$$\mathbf{W} = \begin{pmatrix} \mathbf{W}_{b_1b_1} & \mathbf{W}_{b_1b_2} & \cdots & \mathbf{W}_{b_1b_N} \\ \mathbf{W}_{b_2b_1} & \mathbf{W}_{b_2b_2} & & \vdots \\ \vdots & & \ddots & \vdots \\ \mathbf{W}_{b_Nb_1} & \cdots & \cdots & \mathbf{W}_{b_Nb_N} \end{pmatrix}. \tag{10}$$

The matrix $\mathbf{W}$ thus consists of N^2 submatrices that represent the propagation between two boundaries. The matrix components $\mathbf{W}_{b_xb_x}$ ($x \in [1..N]$) on the diagonal represent the interaction of the boundary with itself. This can be interpreted as propagating bending waves. In general cases these matrices will be zero $\mathbf{W}_{b_xb_x} = \mathbf{0}$, while the interaction of the wall with itself can already be included in the fully occupied $\mathbf{R}$ matrix. Furthermore, it can be easily seen that $\mathbf{W}_{b_xb_y} = \mathbf{W}_{b_yb_x}$, because of reciprocity.

The wave field at the detectors in the case of one first-order reflection at all boundaries is calculated by:

$$\vec{P}_1 = \left[\mathbf{W}_{db}\mathbf{R}\mathbf{W}_{bs}\right]\vec{S}, \tag{11}$$

and if this is extended to the m^{th}-order reflection, Eq. (11) can be generalized to:

$$\vec{P}_m = \left[\mathbf{W}_{db}\left(\mathbf{R}\mathbf{W}\right)^m\mathbf{R}\mathbf{W}_{bs}\right]\vec{S}. \tag{12}$$

The resulting reflected wave field at the detector locations $\vec{P}_{\text{refl}}$ is given by the summation of all reflection orders M, which results in the following equation in case of $M = \infty$:

$$\begin{aligned}\vec{P}_{\text{refl}} &= \sum_{m=0}^{M=\infty}\left[\mathbf{W}_{db}\left(\mathbf{R}\mathbf{W}\right)^m\mathbf{R}\mathbf{W}_{bs}\right]\vec{S} \\ &= \left[\mathbf{W}_{db}\left(\mathbf{I}-\mathbf{R}\mathbf{W}\right)^{-1}\mathbf{R}\mathbf{W}_{bs}\right]\vec{S},\end{aligned} \tag{13}$$

where use is made of the fact that the summation is a Neumann series, which can be written as a matrix inversion. The matrix $\mathbf{I}$ here is the unity matrix. Furthermore, it is necessary to add the direct wave field $\vec{P}_{\text{dir}}$ from the source(s) to the detector(s), schematically shown in the bottom part of Figure 3, to get the total wave field $\vec{P}$ at the detector(s):

$$\begin{aligned}\vec{P} &= \vec{P}_{\text{dir}} + \vec{P}_{\text{refl}} \\ &= \left[\mathbf{W}_{ds} + \mathbf{W}_{db}\left(\mathbf{I}-\mathbf{R}\mathbf{W}\right)^{-1}\mathbf{R}\mathbf{W}_{bs}\right]\vec{S}.\end{aligned} \tag{14}$$

Source directivity

The source directivity is captured in the matrix $\mathbf{D}$, where the elements are weighting factors for the different propagation paths between the source and the boundary $\mathbf{D}_{bs}$ and the source and receivers $\mathbf{D}_{ds}$. These weighting factors are frequency and orientation dependent. This directivity matrix can be included in the WRWes formulation as follows:

$$\begin{aligned}\vec{P} &= \vec{P}_{\text{dir}} + \vec{P}_{\text{refl}} \\ &= \left[\mathbf{W}_{ds}\odot\mathbf{D}_{ds} + \mathbf{W}_{db}\left(\mathbf{I}-\mathbf{R}\mathbf{W}\right)^{-1}\mathbf{R}\mathbf{W}_{bs}\odot\mathbf{D}_{bs}\right]\vec{S}.\end{aligned} \tag{15}$$

Where the symbol $\odot$ indicates an element wise multiplication between two matrices of the same dimensions.

Results

To test the implementation of the directivity in the WRWes algorithm, a simulation of a real source in a square room is compared to a simulation of the same room but with a monopole and the mapped directivity of the original source. The square room has the dimensions of 4x4x4

meters and it has low absorbing walls (reflection factor of $R = 0.97$). The source is built-up from 5 monopole sources with the same source strength, but with different positions and zero phases placed in the center of the room. Their coordinates $[xyz]$ and zero phases ϕ_0 are listed in Table 1. The coordinates are relative to the general center point of the source.

Table 1: Coordinates (relative to the common center point of the monopoles) and zero phases of the 5 monopoles that form the used source.

Nr.	Position & Phase			
	x[m]	y[m]	z[m]	ϕ[rad]
1	-0.085	0	0	0
2	0.085	0	0	π
3	0	0.11	0	$\pi/2$
4	0	-0.11	0	$3\pi/2$
5	0	0	0.1	$\pi/3$

The comparison is done by "measuring" the directivity of the original source (5 monopoles) by a simulation in free field with a spherical receiver array of 65160 receivers, such that an equidistant distribution of the receivers is obtained. The angle between receivers is kept constant at 1 degree and the distance of the source center to the receivers is 1 meter. This "measured" directivity is used as input for the simulation with the monopole and mapped directivity.

The spatial wave fields for both the simulation of both the original source and the monopole with mapped directivity are compared at a receiver plane positioned at $\frac{3}{4}$ height of the room is given in Figure 4 for the frequency of 200 Hz. The spatial image is build-up from the responses of 5776 receiver points with a 0.05 meter spacing.

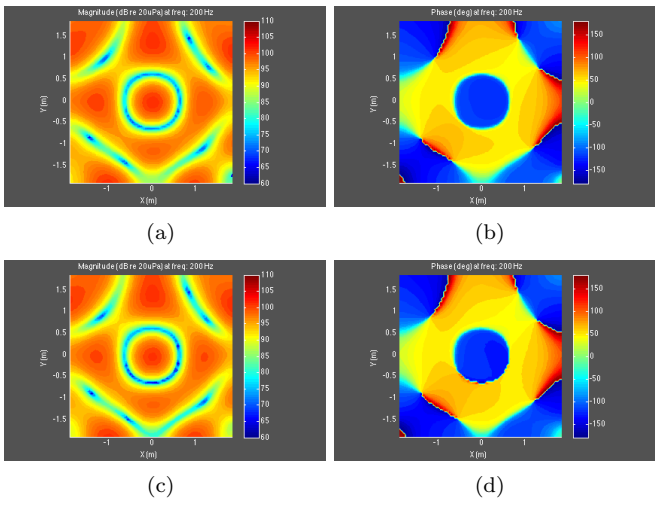

(a) (b)

(c) (d)

Figure 4: Spatial wave field at 200 Hz for the original source (a)&(b) and the monopole source with directivity (c)&(d), with left the magnitude and right the phase.

The frequency and phase responses of both simulations at receiver number 3000 ($[x; y; z] = [0.05; -0.15; 1.00]$) from 50 Hz to 2000 Hz in 20 Hz steps is shown in Figure 5.

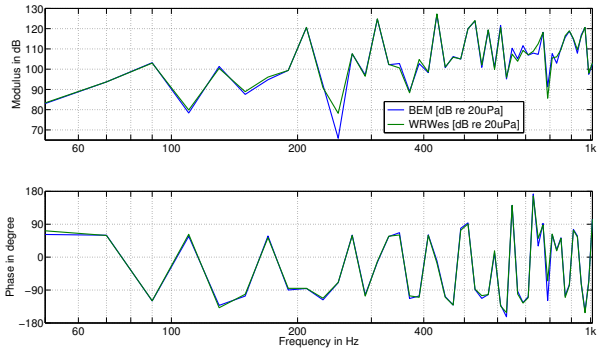

Figure 5: Frequency and phase response in 20 Hz steps for the original source (BEM) and the monopole source with directivity (WRWes).

Discussion and conclusion

A wave based room acoustic simulation method (WRWes) is presented which is able to use measured directivities of sources. The advantage is that a coupled simulation (fluid-structure) can be omitted. Any source directivity can be used for simulations without having a mathematical description. The results show that the method is reliably, but it must be noted that it only works for far field considerations of the source.

References

[1] Opdam, R.: Simulation of non-locally reacting boundaries with a single domain boundary element method. J. Acoust. Soc. Am. (2013), Vol 133.

[2] Opdam, R.: Frequency and geometry dependent automated optimized meshing algorithm for a boundary element simulation. DAGA 2014, (2014).

[3] Berkhout, A.: Seismic migration, imaging of acoustic energy by wave field extrapolation, A. Theoretical aspects. Elsevier Science Publishers B.V., Amsterdam, 1984.